Available online at www.sciencedirect.com
SCIENCE DIRECT®
Journal of Solid State Chemistry 177 (2004) 2053–2057
JOURNAL OF SOLID STATE CHEMISTRY
http://elsevier.com/locate/jssc

Spin-glass like behavior in a new ternary uranium cobalt aluminide, $U_3Co_{4+x}Al_{12-x}$ with $x = 0.55(2)$

O. Tougait,[a,*] H. Noël,[a] and R. Troc[b]

[a] *Laboratoire de Chimie du Solide et Inorganique Moléculaire, UMR 6511 CNRS- Université de Rennes1, Institut de Chimie, Avenue du Général Leclerc, 35042 Rennes, France*

[b] *W. Trzebiatowski Institute of Low Temperature and Structure Research, 50-950 Wroclaw, P.O. Box 1410, Poland*

Received 24 November 2003; received in revised form 23 January 2004; accepted 1 February 2004

Abstract

The new compound $U_3Co_{4+x}Al_{12-x}$, where $x = 0.55(2)$, was prepared by arc-melting of the elemental components, followed by a prolonged annealing at elevated temperature. Scanning electron microscopy-energy-dispersive spectroscopy and powder X-ray diffraction were used to determine the deviation from the ideal stoichiometry. A small homogeneity range, that extends around the composition $U_3Co_{4+x}Al_{12-x}$ with $0.4(1) \leqslant x \leqslant 0.7(1)$, could be detected. Single-crystal diffraction experiments revealed that $U_3Co_{4.55}Al_{11.45}$ crystallizes with the $Gd_3Ru_4Al_{12}$ type-structure, (space group $P6_3/mmc$, $Z = 2$) in a cell of dimensions at room temperature, $a = 8.6518(2)$ Å, $c = 9.2620(2)$ Å. The crystal structure can be viewed as an intergrowth of two distinct layers of Co and Al atoms, and U, Al and mixed Al/Co atoms that pile up along the hexagonal axis. The results of the DC magnetization suggest the occurrence of a spin glass state at low temperature ($T_f = 8$ K). The origin of freezing of the magnetic moments may arise from a topological frustration due to the location of the U atoms on the apexes of a distorted Kagomé lattice.

Keywords: Uranium alloy; Crystal structure; Ternary phase diagram; Frustrated magnetism; Correlated electron system

1. Introduction

New ternary intermetallic compounds containing uranium, a transition metal and an element of the *p*-block have attracted widespread attention for the study of fundamental aspects of magnetism. Examples of complex magnetic behaviors and rich magnetic phase diagrams are legion. For example, they comprise the antiferromagnetic heavy fermion superconductors UNi_2Al_3 and UPd_2Al_3 [1], showing evidence of magnetic order below the superconducting transition, the successive magnetic phases of UPd_2Ge_2 [2], varying upon cooling the temperature from incommensurate to commensurate structures, or the magnetic evolution encountered in the UCu_xSi_{2-x} system [3], moving towards the composition from spin fluctuations through ferromagnetism next to the spin-glass state, and finally to a non-collinear antiferromagnetic structure. It is commonly assumed that the variety of magnetic phenomena of the U-based compounds is due to the specific nature of the 5*f* electrons, which cover a wide range between localized and itinerant behaviors. The degree of delocalization (or localization), which occurs either via the direct overlap of the 5*f*-electron shells of the neighboring U atoms, or the 5*f*-ligand hybridization, governs the magnetic properties.

In the course of our systematic investigation of the U–Co–Al ternary phase diagram, the new ternary compound $U_3Co_{4+x}Al_{12-x}$ was synthesized. The structural analysis showed readily that it adopts the $Gd_3Ru_{4+x}Al_{12-x}$ type-structure [4]. Up to now, a large number of ternary aluminides of rare-earth (*Ln*) and transition metal (*T*) crystallizing with the same type of structure have been reported [5]. They have been prepared with most of the rare-earth elements, including Y, whereas the transition metal is Ru or Os exclusively. The crystal structure refinements show mixed *T*/Al occupancies leading to compositions written as $Ln_3T_{4+x}Al_{12-x}$, where x ranges from 0.06 to 0.44; the ideal occupancy values being not observed to date. In the present article, we report on the synthesis, structural

*Corresponding author. Fax: +33-2-99-38-34-87.
E-mail address: tougait@univ-rennes1.fr (O. Tougait).

0022-4596/$ - see front matter © 2004 Elsevier Inc. All rights reserved.
doi:10.1016/j.jssc.2004.02.009

and chemical analyses as well as the magnetic properties of the new compound $U_3Co_{4.55}Al_{11.45}$.

2. Experimental section

2.1. Syntheses

The metals used were aluminum (ingot, 5N, Strem), cobalt (pieces, 3N, Strem) and uranium (pieces, nuclear grade, Merck). The samples, with a total weight of about 0.5 g, were prepared by reaction of the elements melted in an arc-furnace under argon atmosphere. The cooled buttons were flipped and remelted three times to achieve homogeneity. The weight losses were less than 1 wt%. Each sample was placed into an alumina crucible and sealed in a fused silica tube under a residual atmosphere of argon. They were then heat treated at 1050°C for 500 h using a computer-controlled furnace.

2.2. EDX analysis

Metallographic and quantitative analyses were carried out with the use of a 6400-JSM scanning electron microscope equipped with an Oxford Link Isis spectrometer. The specimens prepared by mounting a piece of each sample in resin were thoroughly polished down to 1 μm before examination. Additional corrections were superimposed to the internal ZAF-type corrections through the use of the stoichiometric compounds UAl_2, UCo_2 and Co_2Al_5 as external standards.

2.3. X-ray diffraction studies

All samples were analyzed by powder X-ray diffraction patterns collected on an INEL CPS 120 diffractometer using a monchromatized Cu$K\alpha_1$ radiation. Comparison of the diffraction patterns with various type-structures was carried out with the help of the program POWDERCELL [6].

The single crystal used for the refinement was manually selected from a sample with starting composition U:Co:Al of 2:3:8 (i.e., 3:4.5:12). The X-ray diffraction experiments were carried out with the use of a Nonius Kappa CCD diffractometer. The unit-cell parameters, orientation matrix as well as the control of the crystal quality were derived from 10 frames recorded at $\phi = 0$ using a scan of 1° in ω. The complete strategy to fill more than a hemisphere was automatically calculated with the use of the program COLLECT [7]. Data reduction and reflection indexing were performed with the program DENZO of the Kappa CCD software package [7]. The scaling and merging of redundant measurements of the different data sets as well as the cell refinement were measured using DENZO. A face-indexed absorption correction was made with the use of the program ANALYTICAL [8]. The structure was solved in the hexagonal space group $P6_3/mmc$ by direct methods using SIR-97 [9]. All structure refinements and Fourier syntheses were carried out with the help of SHELXL-97 [10]. The resultant displacement ellipsoid for the Al(2) atom located on the 6 h Wyckoff position was abnormally small, suggesting a partial substitution of this Al site by Co as it is described in the structural model of $Gd_3Ru_{4+x}Al_{12-x}$ [4]. Final refinements including a secondary extinction, anisotropic atomic displacement parameters for all atoms as well as the occupancy factor for the mixed Co/Al position yielded the formula $U_3Co_{4+x}Al_{12-x}$, where $x = 0.55(2)$. The crystallographic details are summarized in Table 1. Atomic coordinates and equivalent atomic displacement parameters, with their standard deviations, are given in Tables 2 and 3.

2.4. Magnetic measurements

DC magnetic measurements were carried out using an MPMS Quantum Design SQUID magnetometer. Zero-field-cooled (ZFC) and field-cooled (FC) data were obtained in the temperature range 1.9–20 K with applied fields up to 0.3 T. The temperature dependence of the magnetization (FC) was measured in the range 1.9–300 K under a magnetic field of 0.5 T. The magnetiza-

Table 1
Crystal data and structure refinement for $U_3Co_{4+x}Al_{12-x}$

Empirical formula	$U_3Co_{4.55}Al_{11.45}$
Formula weight (g mol^{-1})	1291
Crystal system, space group	Hexagonal, $P6_3/mmc$
Unit cell dimensions (Å,deg)	
	$a = 8.6518(2)$
	$c = 9.2620(2)$
Volume (Å^3)	600.4(1)
Z, Calculated density (g/cm^3)	2, 7.14
Absorption coefficient (cm^{-1})	465
Crystal color and habit	Black, needle-like
Crystal size (mm^3)	$0.1 \times 0.04 \times 0.03$
Theta range for data collection (deg)	2.72 to 34.88
Limiting indices	$-12 <= h <= 13$,
	$-13 <= k <= 11$,
	$-14 <= l <= 14$
Reflections collected/unique	12666 / 537
R_{int}	0.203
Absorption correction	numerical
Max/min. transmission	0.192/0.069
Data/restraints/parameters	537/0/28
Goodness-of-fit on F^2	1.08
R indices[a] $[I > 2\sigma(I)]$	$R(F) = 0.027$,
	$wR_2 = 0.069$
Extinction coefficient	0.0050(5)
Largest diff. peak and hole (e Å^{-3})	3.13/−2.24

$wR2 = \left[\sum w(F_o^2 - F_c^2)^2 / wF_o^4\right]^{1/2}$, where $w^{-1} = [\sigma^2(F_o^2) + 7.27P]$, $P = [\max(F_o^2, 0) + 2F_c^2]/3$.

[a] $R(F) = \sum||F_o| - |F_c||/|F_c|$.

Table 2
Atomic coordinates and equivalent isotropic displacement parameters (Å^2) for $U_3Co_{4+x}Al_{12-x}$

Atom	Wyckoff position	Occupancy	x	y	z	U_{eq}. (Å^2)
U(1)	6*h*	1	0.1980(1)	0.3960(1)	1/4	0.0011(1)
Co(1)	2*a*	1	0	0	0	0.0008(1)
Co(2)	6*g*	1	1/2	0	0	0.0010(1)
Al(1)	12*k*	1	0.1615(1)	0.3230(3)	0.5797(2)	0.0010(1)
Al(2)	6*h*	0.82(2)	0.5643(2)	0.1285(3)	1/4	0.0010(1)
Co(3)	6*h*	0.18(2)	0.5643(2)	0.1285(3)	1/4	0.0010(1)
Al(3)	4*f*	1	1/3	2/3	0.0082(4)	0.0010(1)
Al(4)	2*b*	1	0	0	1/4	0.0012(1)

U_{eq} is defined as one third of the trace of the orthogonalized U_{ij} tensor.

Table 3
Selected interatomic distances (Å) for $U_3Co_{4+x}Al_{12-x}$

U(1)–Al(4)	2.967(1)	Co(1)–Al(4) × 2	2.316(1)	Al(1)–Co(1)	2.530(2)
U(1)–Al(2) × 2	3.012(2)	Co(1)–Al(1) × 6	2.530(2)	Al(1)–Co(2) × 2	2.642(1)
U(1)–Al(3) × 2	3.021(3)			Al(1)–Al(3)	2.701(2)
U(1)–Al(1) × 2	3.103(2)	Co(2)–Al(3) × 2	2.499(1)	Al(1)–Al(2) × 2	2.743(2)
U(1)–Al(1) × 4	3.157(2)	Co(2)–Al(2) × 2	2.508(1)	Al(1)–Al(1) × 2	2.835(3)
U(1)–Co(2) × 4	3.263(1)	Co(2)–Al(1) × 4	2.642(1)	Al(1)–Al(4)	2.889(2)
U(1)–U(1) × 2	3.512(2)	Co(2)–U(1) × 4	3.263(1)	Al(1)–U(1)	3.103(2)
				Al(1)–U(1) × 2	3.157(2)
Al(2)–Co(2) × 2	2.508(1)	Al(3)–Co(2) × 3	2.499(1)	Al(4)–Co(1) × 2	2.316(1)
Al(2)–Al(2) × 2	2.658(4)	Al(3)–Al(1) × 3	2.701(2)	Al(4)–Al(1) × 6	2.889(2)
Al(2)–Al(1) × 4	2.743(2)	Al(3)–Al(2) × 3	2.841(3)	Al(4)–U(1) × 3	2.967(1)
Al(2)–Al(3) × 2	2.841(3)	Al(3)–U(1) × 3	3.021(3)		
Al(2)–U(1) × 2	3.012(2)				

tion was measured at 1.9 K in increasing and decreasing magnetic fields up to 5 T. All the physical measurements were performed on samples with the initial composition $U_3Co_{4.55}Al_{11.45}$.

3. Results and discussion

3.1. Characterization and crystal structure description

Initial investigations of the ternary U–Co–Al system were carried out by analyzing samples with diverse starting compositions. The existence of the new phase $U_3Co_{4+x}Al_{12-x}$ was revealed by X-ray powder diffraction and SEM-EDX analyses. A small homogeneity range $0.4 < x < 0.7$ was indicated by the EDX analyses. It is worthwhile mentioning that the present phase is intrinsically disordered; the ideal composition $U_3Co_4Al_{12}$ has not been observed. A rationale for this, may be ascribed to the occurrence of another phase, $U_2Co_3Al_9$ (U(14.3); Co(21.4); Al(64.3)) crystallizing with the $Y_2Co_3Ga_9$ type of structure [11] which has atomic ratios extremely close to those calculated from the formulae $U_3Co_4Al_{12}$ (U(15.79); Co(21.05); Al(61.16)).

The $Gd_3Ru_4Al_{12}$-type structure in which the present compound crystallizes has been described in detail several times in the literature [4,5]. A perspective view of the crystal structure is displayed in Fig. 1; for clarity all the bonds are not displayed. The crystal structure of $U_3Co_{4+x}Al_{12-x}$ may be considered as an intergrowth of two kinds of layers that alternate along the *c*-direction. The layers of the first kind contain the Co(1), Co(2), Al(1) and Al(3) atoms that are almost hexagonally close-packed. These layers, which are slightly puckered, lie at $z = 0$ and $z = \frac{1}{2}$. The atoms U(1), Al(4) and the mixed Al(3)/Co(2) atoms lie in the second kind of layers which are located at $z = \frac{1}{4}$ and $z = \frac{3}{4}$. Within these planes, the U atoms are located on the apexes of triangles of two different sizes, defining a slightly distorted Kagomé net (Fig. 2). The larger triangles centered by an Al(4) atom have an edge length of 5.14(1) Å, whereas the smaller triangles have an edge length of 3.512(2) Å.

Selected interatomic distances (up to 3.60 Å) together with the number of near neighbors are given in Table 3. All the Co–Co interatomic distances are longer than 4.20 Å. Considering the sum of the atomic radii (1.25 Å for Co, 1.43 Å for Al and 1.53 Å for U) as a criterion to evaluate the strength of the chemical bonds, interactions between the atomic components within the

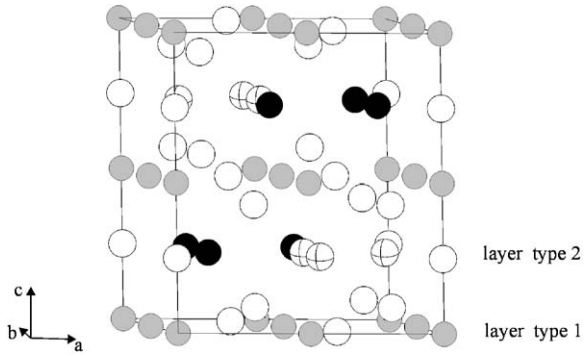

Fig. 1. Perspective view of $U_3Co_{4.55}Al_{11.45}$. Black circles represent the U atoms, white ones the Al atoms, gray ones the Co atoms and the crossed circles are the mixed Al/Co atoms.

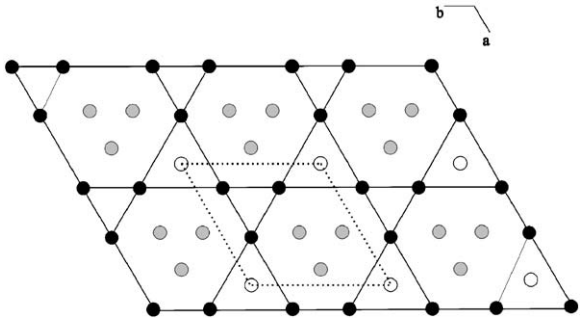

Fig. 2. Projection into the $a-b$ plane of the second kind of layer constituting the crystal structure of $U_3Co_{4.55}Al_{11.45}$. Black circles represent the U atoms, white ones the Al atoms and gray ones the mixed Al/Co atoms. The solid lines give the schematic drawing of the Kagomé net. The dashed lines are the projection of the unit-cell.

$U_3Co_{4+x}Al_{12-x}$ structure may be classified into two groups. Uranium has a coordination number of 17, composed of eleven Al atoms, four Co atoms and two U atoms; all the interatomic distances around the U atom are above the sum of the atomic radii, precluding any strong bonding interactions between U and its near-neighbor atoms. In contrast, the Co–Al and Al–Al distances, with the exception of the Al(1)–Al(4) contact of 2.889(2) Å, are well below the sum of the atomic radii, suggesting rather strong Co–Al and Al–Al bonding interactions. A similar examination of the bond lengths in the ternary aluminides $Ln_3T_{4+x}Al_{12-x}$ [4,5] where *Ln* is a rare-earth element and *T* is Ru or Os reveals a different feature. The *Ln*–Al, *T*–Al and Al–Al interatomic distances are found to compare well to the sum of the corresponding metallic radii, leading to close-packed structures.

3.2. Magnetic properties

Fig. 3 gives the thermal dependence of the inverse DC magnetic susceptibility of $U_3Co_{4+x}Al_{12-x}$ measured for temperatures between 1.9 and 300 K. Least-squares

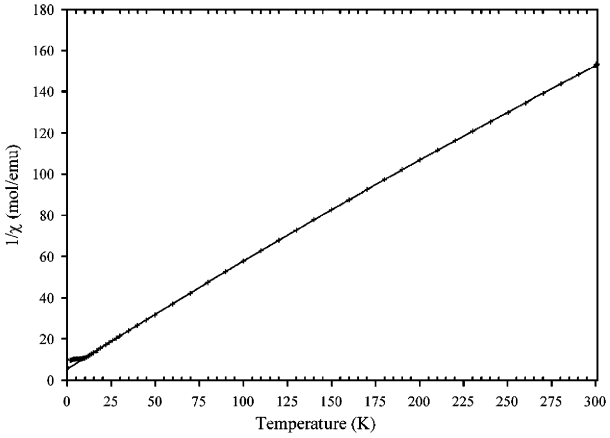

Fig. 3. Inverse of the thermal DC magnetic susceptibility measured under zero-field-cooled condition and with an applied field of 5 kGs. The solid line represents the Curie–Weiss fit of the data.

fitting of these data taken in the temperature range 20–300 K to the modified Curie–Weiss law ($\chi = C/(T-\theta_p)+\chi_0$) leads to an effective magnetic moment per uranium atom $\mu_{eff} = 2.70(1)\,\mu_B$/U atom, a paramagnetic Curie temperature $\theta_p = -10(1)$ K and an independent term $\chi_0 = 6.10^{-4}$ emu/mol. The obtained value of the effective magnetic moment compared to those calculated for the U^{3+} and U^{4+} ions, assuming a Russel–Saunders coupling ($\mu_{eff}(U^{3+}) = 3.62\,\mu_B$ and $\mu_{eff}(U^{4+}) = 3.58\,\mu_B$) suggests a certain delocalization of the 5*f*-electons, and crystal electrical field interactions. For temperatures below 6 K, the experimental points deviate from the fitting curve, suggesting some magnetic correlations, probably of antiferromagnetic type, indicated by the negative value of the paramagnetic Curie temperature ($\theta_p = -10(1)$ K).

Fig. 4 gives the thermal evolution of the magnetic susceptibility ($\chi_{dc} = M/H$) for the ZFC and FC conditions recorded under various applied fields (20, 100, 200, 500, 1000 and 3000 Gs). A pronounced cusp is observed on the ZFC curves at a temperature close to 8 K at low fields. At higher applied fields, this cusp transforms to a rounded maximum. The separation between the ZFC and FC susceptibility curves at the cusp temperature indicates more likely the characteristic features of a spin-glass behavior. This irreversibility may be ascribed to different arrangements of the magnetic moments below the freezing temperature T_f, which corresponds to the temperature at which the ZFC and FC curves start to separate. It is interesting to note that upon increasing the applied field up to 0.1 T, the shift of T_f toward low temperatures is negligible. However, a distinct shift amounting to about 2 K is observed when the magnetic field increased from 0.1 to 0.3 T. Another intrinsic feature of spin-glass behavior is the deviation from a straight line and the weak hysteresis effect

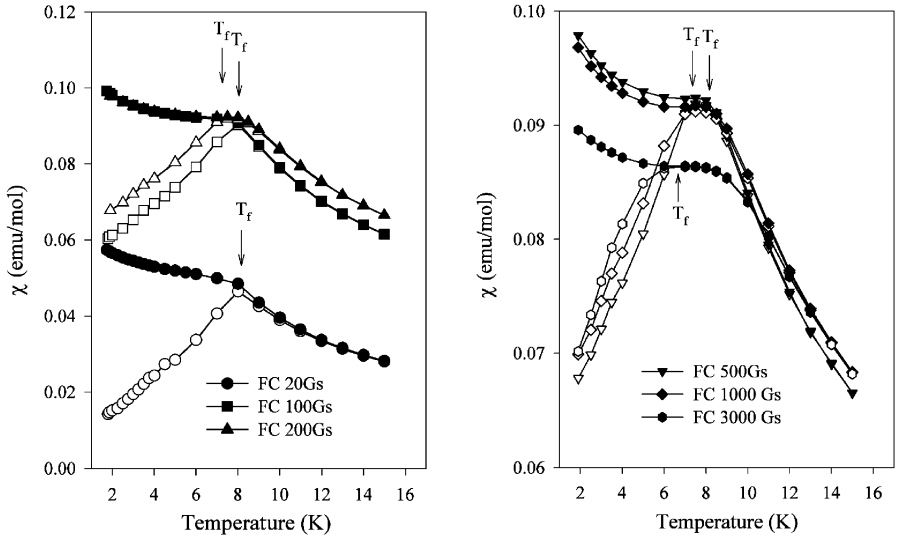

Fig. 4. Low-temperature details of the DC magnetic susceptibility of $U_3Co_{4.55}Al_{11.45}$ recorded for various applied fields (20, 100, 200, 500, 1000 and 3000 Gs) and after zero field cooling (ZFC) and field-cooling (FC). The empty symbols represent the ZFC and the filled symbols the FC.

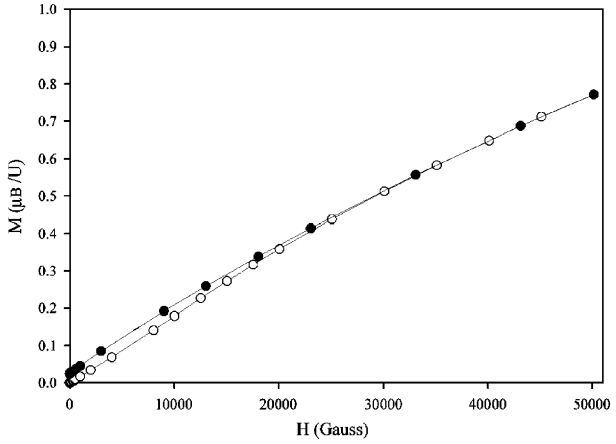

Fig. 5. Magnetic field dependence of the magnetization of $U_3Co_{4.55}Al_{11.45}$ at 1.9 K.

observed in the field dependence of the magnetization. These features are displayed in Fig. 5. The remanent magnetization is found to be about 0.024 μ_B per U atom at 1.9 K.

Finally, the spin-glass state at low temperature in $U_3Co_{4.55}Al_{11.45}$ compound is strongly supported by geometrical considerations. The uranium sublattice comprises a two-dimensional triangular net, defined as a Kagomé lattice, which is one of the best-known examples for topological frustration. Further physical measurements including AC susceptibility, heat capacity and transport properties are in progress, in order to fully characterize the low temperature behavior of this new ternary aluminide.

Acknowledgments

This work was partially supported by the exchange program between CNRS and Polish Academy of Sciences, under the project 6386. Use was made of the Nonius Kappa CCD diffractometer through the Centre de Diffraction X de l'Université de Rennes1 (CDIFX).

References

[1] C. Geibel, A. Böhn, R. Caspary, K. Gloos, A. Grauel, P. Hellmann, R. Modler, C. Schank, G. Weber, F. Steglich, Physica B 186–188 (1993) 188–194.
[2] G. André, F. Bourée, A. Oleœ, W. Sikora, B. Pene, A. Szytuła, Z. Tomkowicz, Solid State Commun. 97 (1996) 923–929.
[3] S. Pechev, T. Roisnel, B. Chevalier, B. Darriet, J. Etourneau, Solid State Sci. 2 (2000) 773–780.
[4] R.E. Gladyshevskii, O.R. Strusievicz, K. Cenzual, E. Parthé, Acta Crystallogr. B 49 (1993) 474–478.
[5] J. Niermann, W. Jeitschko, Z. Anorg. Allg. Chem. 628 (2002) 2549–2556.
[6] W. Krause, G. Nolze, Federal Institute for Materials Research and Testing, Berlin, Germany.
[7] Nonius, in: Collect, Denzo, Scalepack, Sortav, Kappa CCD Program Package, Nonius BV, Delft, The Netherlands, 1998.
[8] A. Altomare, M.C. Burla, M. Camalli, G.L. Cascarano, C. Giacovazzo, A. Guagliardi, A.G.G. Moliterni, G. Polidori, R. Spagna, J. Appl. Crystallogr. 32 (1999) 115–119.
[9] J. de Meulenaar, H. Tompa, Acta Crystallogr. A 19 (1965) 1014.
[10] G.M. Sheldrick, Shelxs97 and Shelxl97, University of Göttingen, Germany.
[11] Yu.N. Grin', R.E. Gladyshevskii, O.M. Sinevich, V.E. Zavodnik, Ya.P. Yarmolyuk, I.V. Rozhdestvenskaya, Sov. Phys. Crystallogr. 29 (1984) 528.